Simulation of Metal Cutting using Smooth Particle Hydrodynamics

Morten F. Villumsen[1], Torben G. Fauerholdt[2]

[1]Bang & Olufsen, Struer, Denmark
[2]Aalborg University, Department of Production, Aalborg, Denmark

Summary:

The purpose of this study is to introduce an approach of metal cutting simulation. A Smooth Particle Hydrodynamics (SPH) based model is carried out using the LS-DYNA software. SPH is a meshless method which is very promising as a numerical method for modelling problems involving large deformations such as metal cutting. Predicted cutting forces are compared with results from experiments. Series of sensitivity analyses were performed in order to evaluate the SPH based model. The model's sensitivity to changes of different parameters was examined. Experimental measuring of the cutting forces was performed with Kistler dynanometer type 9257BA. The numerical simulations were performed with the explicit finite element code LS-DYNA Ver. 971. rev. 7600.1224.
A good agreement between the predicted and measured cutting forces was observed. The chip formation was also predicted well. The results of the analyses are: the cutting force was underestimated by 8.4% and the thrust force was underestimated by 12% when compared with measured forces from experiments.

Keywords:

Metal cutting, Smooth Particle Hydrodynamics, numerical prediction of cutting forces, LS-DYNA, experimental measurement of cutting forces

1 Introduction

1.1 Bang & Olufsen's Motivation

Since the 1960s Bang & Olufsen has used aluminium in their products. Aluminium is used as a design feature to express excellence in the luxury high-end audio and video products. The surface of the aluminium is very essential in expressing this. The processes used for the manufacturing of these aluminium surfaces are: grinding, polishing and metal cutting (milling and turning). All parts with surfaces produced by these processes are subsequently anodized in order to obtain a scratch-resistant surface. These processes are among the core competencies at Bang & Olufsen.
The metal cutting processes such as milling and turning produce surfaces without any other after-treatment than the anodizing process, and these milled and turned surfaces are visible on the final Bang & Olufsen products. Therefore it is of extreme importance that surface errors are reduced to an absolute minimum.
The workpieces must be clamped and fixed during machining. Clamping of the workpieces in the machines became a vital issue lately. The clamping fixtures are very complex and very costly if all the demands on the surface are to be met. It is of high importance to minimize vibrations, surface and geometrical errors, and thereby reduce the production costs.
 In order to meet these demands and to continuously develop the metal cutting process, better modelling is necessary in order to predict cutting forces. At Bang & Olufsen we are working with

steady improvement of the competencies within the field of metal cutting, and this work should contribute to a higher level of understanding the metal cutting process.

1.2   Metal Cutting

Metal cutting is one of the most used production processes in the industry. The process is very flexible and can be used for production of parts with complex geometry and fine tolerances. Despite of the importance of this process, it is one of the production processes least examined. Furthermore, process parameters are still mainly chosen based on empirical knowledge. Experimental investigations are costly and time demanding and even though material databases with a large number of material and tool combinations exist, the experimental investigations show that these databases loose their relevance as new materials, tools and new and faster machines are developed. Thus, a better analysis of the cutting process is necessary in order to select cutting tools and process parameters.

1.3   Analysis of Metal Cutting

Researchers have developed a large number of models for the metal cutting process during the last 60 years. As an example Kienzle [12] develops an empirical model based on a large number of experiments; Merchant [16], Armarego and Brown [10] and Oxley [14], develop analytical models. Within recent years mainly Finite Element Methods are used to simulate the metal cutting process, Massilimani [1], Raczy et al. [2] and Olovsson [19]. Improvements of manufacturing technologies such as metal cutting require better modelling and analysis. Numerical methods became recently an efficient tool for investigation of the complex phenomenon: metal cutting. The FE technique as a method for analysing metal cutting is a novel approach and hopefully it can contribute to a higher level of understanding this process. A more in-depth understanding is important for selecting cutting tools and process parameters.

However, it is a complex process which requires a metaphysic approach in order to handle the combined effects of material nonlinear behaviour, geometrical nonlinear behaviour and thermo mechanical effects.

1.4   Numerical Methods

Lagrangian and Euler techniques are typical approaches in the analysis of metal cutting as well as a combination of both - Arbitrary Lagrangian Euler (ALE). Furthermore, the Smooth Particle Hydrodynamics (SPH) method is used.

The main difference between Lagrangian and Euler methods is that the discrete mesh is coupled to the part and the material for the Lagrangian method; whereas the Euler method assumes that the material floats through a mesh controlled volume. In the ALE method the mesh does not need a coupling to the material, but can move arbitrarily. The mesh is moved during calculation to optimize the element form independently of the material deformation.

Smooth Particle Hydrodynamics (SPH) does not have a mesh as Lagrangian, Euler and ALE. Instead of a mesh the model is defined by a number of mesh-points (particles) with a field around them as shown in Fig. 1. The method was originally developed for problems in astrophysics, but it has been improved during the last decade. This method is used today in fluid and continuum mechanics, mostly Hypervelocity impact analysis, Michel et al. [24], Li et al. [25] and Chen et al. [26], but full potential of the SPH method is not yet examined in-depth.
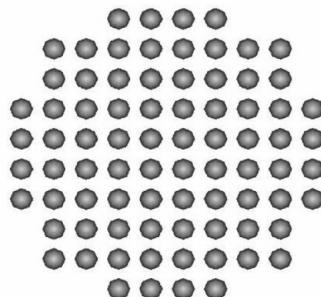
Fig. 1. Example of SPH mesh, Hallquist [21]

Strenkowski and Carroll [11] use the Lagrangian method with a model where a failure surface is predefined, see Fig. 3. In the cutting process both the material and the chip in the area of the tool tip yield, see Fig. 2. However, the fracture area at the tool tip is not well modelled using a failure surface. Therefore Lagrangian models without a predefined failure surface give a more realistic material flow. In these models the tool separates the material and the chip and then simulates the chip formation as shown in Fig. 2. Masillamani et al. [1] use a Lagrangian method in the FEM code LS-DYNA. The cutting temperature is examined in the models. Masillamani et al. achieve good agreement between temperatures from analysis and temperatures measured from tests.
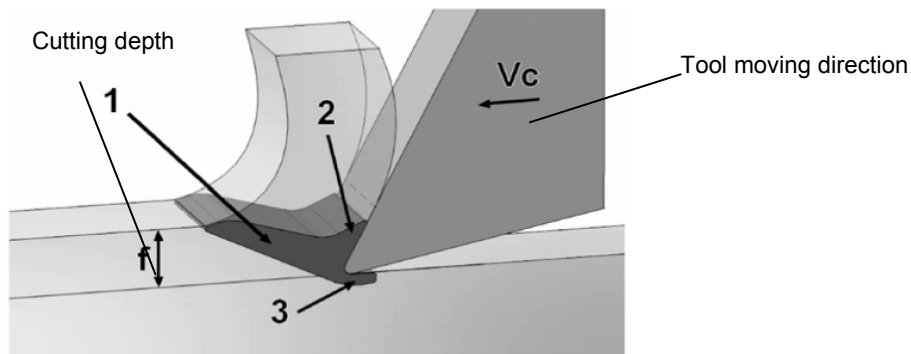
Fig. 2. The three plastic zones in metal cutting,
 1 The primary zone, 2 the secondary zone, 3 the tertiary zone, Limido et al. [3]
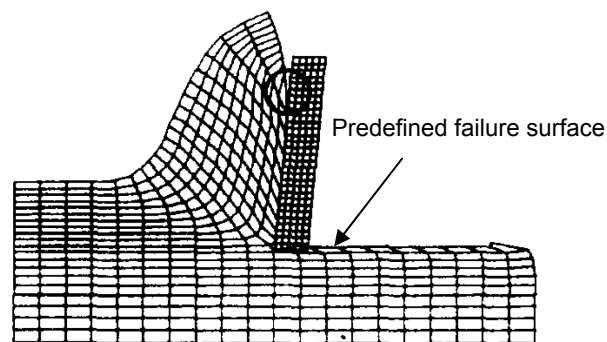
Fig. 3. Lagrangian element method with a
predefined failure surface, Strenkowski and Carroll
[11]

Raczy et al. [2] use an Euler method to analyse the metal cutting process with the FEM code LS-DYNA. A good agreement between predicted chip formation and measured chip formation is achieved. Cutting forces from the analysis are also compared with the cutting forces measured from tests. The cutting force is examined for two material models: the Hydrodynamics material model where the cutting force is overestimated by 13% and the Johnson-Cook material model where the cutting force is overestimated by 21%. For the definition of cutting forces see Fig. 4.

Tool moving direction

Chip

α

tool

V_c

$F_y,$

$F_x,$

β

Workpiece
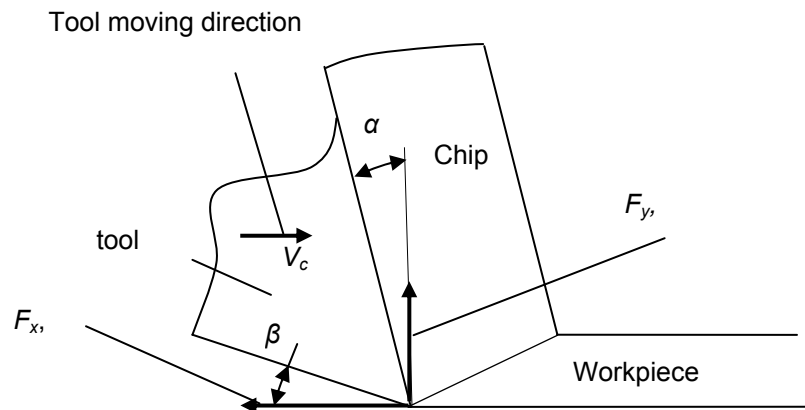
Fig. 4. *Orthogonal cutting forces and angles, α: rake angle, β: relief angle, F_x : The cutting force, F_y: The thrust force, V_c: cutting speed*

The ALE method is used by Olovsson et al. [19] to analyse the metal cutting process where the goal is to predict chip formation. A few test simulations show promising results and the ALE formulation seems numerically robust.

Limido et al. [3] perform a 2D analysis with the SPH method in the FEM code LS-DYNA. Chip formation from analysis is compared to chip formation from tests and good agreement is reported. Moreover, cutting forces from experiments are also compared with cutting forces from analysis. The difference between the predicted and measured forces is 10% for the cutting force and 30% for the thrust force. These results are achieved using the Johnson-Cook material model, see Fig. 5.

1.5 Material Models

Fang [5] performs sensitivity analyses of the flow stress of 18 different materials based on the Johnson-Cook material model. The effects of strain hardening, strain rate hardening and temperature

Time =   4.1999
Contours of Effective Plastic Strain
min=0, at elem# 1000013
max=19.1116, at elem# 2150510

Fringe Levels

1.200e+00
1.080e+00
9.600e-01
8.400e-01
7.200e-01
6.000e-01
4.800e-01
3.600e-01
2.400e-01
1.200e-01
0.000e+00
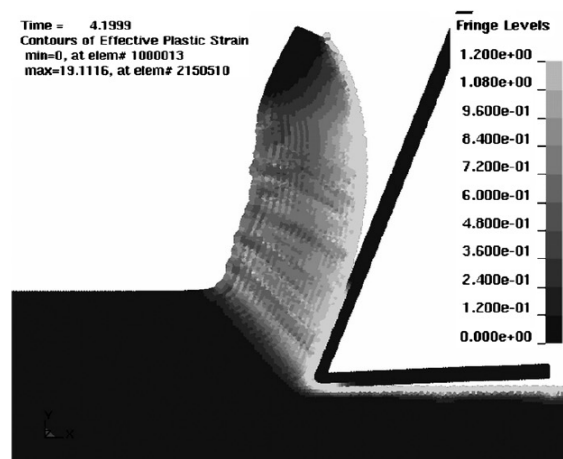
Fig. 5. Result from SPH analysis, showing the effective plastic strain, Limido et al. [3]

softening on the material flow stress are examined. Fang concludes that strain-rate hardening is the least important factor governing the material flow stress, especially when machining aluminium alloys. In addition results for a few material types from the Johnson-Cook material model are compared with results from Oxley [14], Zerilli-Armstrong [17] and Maekawa's [18] material models.

Özel and Karpat [6] determine parameters for the Johnson-Cook material model by using "Co-Operative Swarm Optimization" (CPSO). CPSO is an optimization method here used to determine the material parameters by an inverse technique. The results are compared with other solutions, where material parameters are determined in a traditional way. Özel and Karpat achieve a better agreement

with CPSO results than the results determined in a traditional way, when data is compared with data from experimental tests. According to Özel and Karpat the method can also be used with other material models.

Sedeh et al. [7] extend Oxley's [14] analytical machining theory. Oxley's original theory treats only carbon steels. Sedeh et al. extend the theory to include also copper and aluminium. The theory for Oxley's original material model is compared with Johnson-Cook [9] and Maekawa [18] material models. Sedeh et al. conclude that Johnson-Cook and Maekawa models are better for predicting of cutting forces and temperature compared to experimentally achieved results than Oxley's original model. Jaspers [8] examines the Johnson-Cook and the Zerilli-Armstrong material models for both steel and aluminium. Jaspers compares the two material models and concludes that the mechanical material behaviour is so complex that it is not yet described accurately enough. It is insufficient to look only at flow stress as function of strain, stain rate and temperature. Jaspers concludes that the material models ought to be developed further, so that other parameters such as the material's micro-structure, like crystal orientation and size, as well as the solubility of the alloying elements are also taken into consideration.

1.6   Friction Models used in Analysis of Metal Cutting

Raczy et al. [2] and Sartkulvanich et al. [4] examine the area of friction modelling in metal cutting. The typical friction models used in analysis of metal cutting are coulomb friction and the shear friction model. The friction coefficient is in most cases a value, which is adapted to experimental data by a parameter study. This is for instance carried out in the following ways: Raczy et al. [2] carry out a parameter variation on the coulomb-friction by comparing chip geometry from experiments and from FEM analysis. Sartkulvanich et al. [4] perform a sensitivity analysis of the friction by a parameter variation of the friction coefficient where cutting forces from experiments are compared with force output from FEM analysis. Limido et al. [3] use the SPH method in LS-DYNA and achieve to predict the cutting forces with a 10 % deviation of the cutting force and a 30 % deviation of the thrust force compared to the experimental data. In the SPH method, when using SPH/SPH contact, the friction is modelled as particles interactions, and the friction parameter does not have to be defined. When using SPH/FEM coupling a friction parameter must be defined. Friction modelling in SPH must be studied in-depth but it offers a very interesting alternative to traditional definitions, Limido et al. [3].

2 The Smooth Particle Hydrodynamics Method

The SPH method easily handles large strains which occur in the metal cutting process. The SPH method also handles the separation of chip/workpiece in a more natural manner than the Lagrangian FE model. It is not necessary to use a fracture model n the SPH method. The separation of the particles is implemented in the SPH method. Material data for the *MAT_JOHNSON_COOK material model in LS-DYNA is available for the material used in this work. These material data are adapted from Jaspers [8] and because the SPH method does not need fracture parameters, all material parameters for the material used in this work, are available.

2.1   LS-DYNA / SPH Theory

The Smooth Particle Hydrodynamics (SPH) is an N-body integration scheme developed by Lucy [28], Monaghan and Gingold [20]. The method was developed to avoid the limitations of mesh tangling and distortion in extreme deformation problems with the Finite Element Method. The main difference between the FEM and the SPH method is the absence of a grid. In the SPH method the model is defined by a number of particles. The particles are the computational framework on which the governing equations are resolved.

This method based on the theory in Hallquist [21] is described briefly below.

2.1.1 SPH Formulation:

The particle approximation of a function is:

$$\Pi^h f(x) = \int f(y) W(x-y,h) dy \quad (1)$$

where *W* is the kernel (or smoothing) function.

The kernel function is defined using the function *θ* by the relation:

$$W(x,h) = \frac{1}{h(x)^d} \theta(x) \quad (2)$$

where d is the number of space dimensions and h is the so-called smoothing length which varies in time and space.

$W(x,h)$ should be a centrally peaked function. The most common smoothing kernel function used along with SPH is the cubic B-spline which is defined by choosing θ as:

$$\theta(u) = C \times \begin{cases} 1 - \dfrac{3}{2}u^2 + \dfrac{3}{4}u^3 \ for \left|u\right| \le 1 \\ \dfrac{1}{4}(2-u)^3 \ for \, 1 \le \left|u\right| \le 2 \\ 0 \ for \, 2 < \left|u\right| \end{cases} \qquad (3)$$

Where C is a constant of normalization which depends on the number of spatial dimensions, and u=r/h, r is the distance between two particles, h is the smoothing length, see Fig. 6
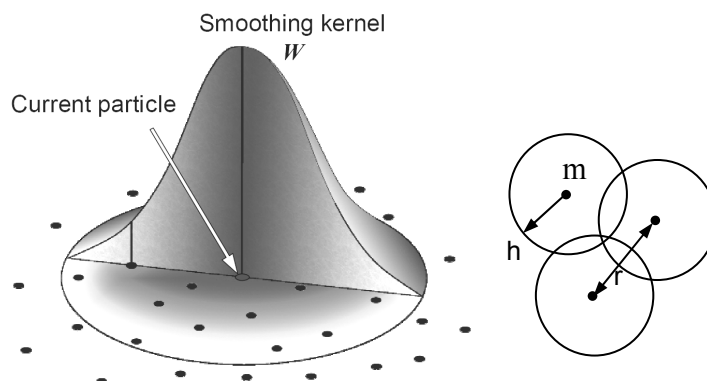
Fig. 6. SPH left) The smoothing kernel (function), right) Typical lengths in the particle model, m: mass, r: distance between particles, h: the smoothing length

The SPH method is based on a quadrature formula for moving particles $((x_i(t))$ $i \in \{1..N\}$, where $x_i(t)$ is the location of the particle i which moves along the velocity field v. The particle approximation of a function can now be defined by:

$$\Pi^h f(x) = \sum_{j=1}^{N} w_j f(x_i) W(x_i - x_j, h) \quad (4)$$

where $\quad w_j = \dfrac{m_j}{\rho_j} \quad (5)$

is the "weight" of the particle. m_j is the mass of the particle j and ρ_j is the density of the particle j.

The weight of a particle varies proportionally to the divergence of the flow. The SPH formalism implies a derivate operator. A particle approximation for the derivative operator must be defined. Before giving the definition of this approximation, the gradient of a function is defined as:

$$\nabla f(x) = \nabla f(x) - f(x)\nabla l(x) \quad (6)$$

where l is the unit function.

Starting from this relation, the particle approximation to the gradient of a function can be defined:

$$\Pi^h \nabla f(x_i) = \sum_{j=1}^{N} \dfrac{m_j}{\rho_j} \big[f(x_j)A_{ij} - f(x_i)A_{ij} \big] \quad (7)$$

where

$$A_{ij} = \dfrac{1}{h^{d+1}} \theta'(\dfrac{\left\|x_i - x_j\right\|}{h}) \quad (8)$$

Discrete form of Conservation Equations
A solution is required for the equation:

$$L_v(\phi) + div F(x, t, \phi) = S \quad (9)$$

where $\phi \in R^d$ is the unknown, F^β with $\beta \in \{1..d\}$ represents the conservation law and L_v is the transport operator defined by:

$$L_v : \phi \longrightarrow L_v(\phi) = \frac{\partial \phi}{\partial t} + \sum_{l=1}^{d} \frac{\partial(v^l \phi)}{\partial x^l} \quad (10)$$

The formulation approximation
In the search of the strong solution the equation can be written, but the strong form is not conservative; therefore this formulation is numerically unacceptable. Thus LS-DYNA is compelled to use the weak form, in the weak form the adjoint of the L_v operator is used:

$$L_v^* : \phi \longrightarrow L_v^*(\phi) = \frac{\partial \phi}{\partial t} + \sum_{l=1}^{d} v^l \frac{\partial \phi}{\partial x^l} \quad (11)$$

The discrete form of this operator corresponds to the discrete formulation of the adjoint of $D_{h.s}$:

$$D_{h,s}{}^* \phi(x_i) = \sum_{j=1}^{N} w_j (\phi(x_i) A_{ij} - \phi(x_j) A_{ji}) \quad (12)$$

A discrete adjoint operator for the partial derivative is also necessary and is taken to be with the *α-th* component of the operator:

$$D^* \phi(x_i) = \sum_{j=1}^{N} w_j \phi(x_j) A^\alpha(x_i, x_j) - w_j \phi(x_i) A^\alpha(x_j, x_i) \quad (13)$$

These definitions are leading to a conservative method. Hence, all the conservative equations encountered in the SPH method will be solved using the weak form.
Applications to conservation equations
With the definitions above, the conservation equations can be written in their discrete form.
For example the equation of conservation of mass is:

$$\frac{d\rho}{dt} = -\rho div(v) \quad (14)$$

which can be evaluated with the following SPH approximation:

$$\frac{d\rho}{dt}(x_i) = \sum_{j=1}^{N} m_j (v(x_j) - v(x_i)) A_{ij} \quad (15)$$

The SPH momentum equation may be written as:

$$\frac{dv^\alpha}{dt}(x_i) = \sum_{j=1}^{N} m_j \left(\frac{\sigma^{\alpha,\beta}(x_i)}{\rho_i^2} A_{ij} - \frac{\sigma^{\alpha,\beta}(x_j)}{\rho_j^2} A_{ji} \right) \quad (16)$$

where *α* and *β* are the space indices
and the energy equation is:

$$\frac{dE}{dt}(x_i) = -\frac{P_i}{\rho_i^2} \sum_{j=1}^{N} m_j (v(x_j) - v(x_i)) A_{ij} \quad (17)$$

Sorting/ neighbour search
In the SPH method the location of neighbouring particles is important. It is very important to know which particle is going to interact with which other at any time of the calculation. The sphere of influence of each particle is a finite domain of a radius *2h* (2 times the smoothing length), see Fig. 7. The goal of the neighbour search is to list the particle inside that domain at each time step. The idea of the search for neighbours is to use the same algorithm as the one used for contact search, namely bucket search. The domain covered by the particles is split into several boxes of a given size, see Fig. 7. This method reduces the number of distance calculations and therefore the computable time is reduced.
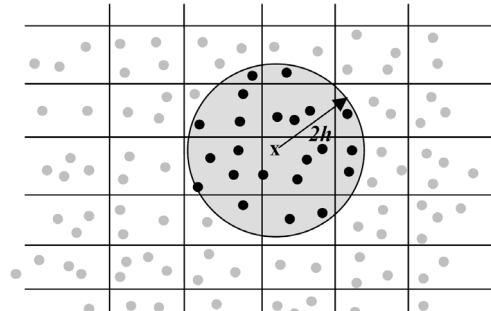
Fig. 7. Bucket sort and neighbour search,
Lacome [23]

An integration cycle in time can be represented by the following SPH calculation cycle in Fig. 8.
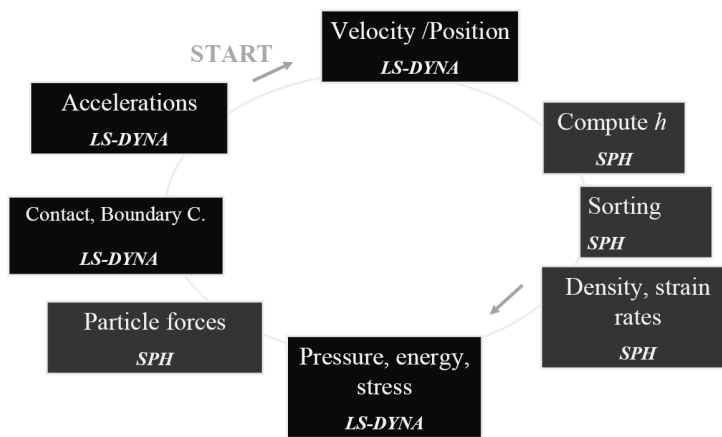
Fig. 8. The calculation cycle for SPH in LS-DYNA, Lacome [22]

3 The Johnson Cook Constitutive Material Model

The Johnson Cook material model [9] was originally developed for penetration analysis, however the material model has become widely used because of its numerical stability. The Johnson Cook material model is already implemented in many FE codes, which is another reason for the widespread use.

Basically the advantage of an analytical model over a purely empirical method is, that for a new material the experimental data required to determine the dependence of flow stress on temperature, strain and strain rate, can be strongly reduced. Ideally, theoretical relationships derived from the physical processes at the atomic level should be used to describe the macroscopic flow behaviour of materials. However, a soundly based theoretical approach of good accuracy is still some way from being realised Jaspers [8]. Consequently, it is inevitable that semi-empirical models are used to describe the constitutive behaviour of materials. One of these constitutive material models is the Johnson-Cook material model.

If ε_p is the equivalent plastic strain, the von Mises flow stress σ is according to the Johnson-Cook model [9]:

$$\sigma = (A + B \cdot \varepsilon_p^{\ n}) \cdot (1 + C \cdot \ln(\dot{\varepsilon}^*)) \cdot (1 - T^{*m}) \quad (18)$$

Where:
A is the material yield stress
B and n are strain hardening parameters
C is a strain rate parameter

$\dot{\varepsilon}^*$ is the homologous plastic strain rate
$$\dot{\varepsilon}^* = \frac{\dot{\varepsilon}}{\dot{\varepsilon}_0} \quad (19)$$

$\dot{\varepsilon}$ is the plastic strain rate

$\dot{\varepsilon}_0$ is the calibration strain rate

m is a temperature coefficient

T^* *is the homologous temperature* $T^* = \dfrac{T - T_{room}}{T_{melt} - T_{room}}$ (20)

T is the real temperature
T_{room} is the room temperature
T_{melt} is the melting point of the specific alloy

3.1   Identification of Parameters for the Johnson-Cook Material Model

Since the strains found in the cutting process are relatively large, it is necessary that the strains achieved in the material tests are of the same order. This means, that as a deformation mode tension test cannot be used due to problems associated with preliminary necking. Thus, the method of loading in the material test should be either torsional or compressive.
The most commonly used test method for determine material parameters for the Johnson-Cook material model is by using the Split Hopkinson Pressure Bar Test (SHPB).
The SHPB test is typically used, in the area strain rates from 200-10.000 (s^{-1}).
To determine the material parameters for the Johnson-Cook material model it is necessary to carry out a number of experiments in the specific material alloy.
To determine the stress/strain parameters, a number of tests are carried out. The tests are performed at varies strain rates and temperatures. The tests are performed with the test equipment as shown in Fig. 9.
The test equipment is build of a "striker bar" and two long slender bars "Incident bar" and "Transmitter
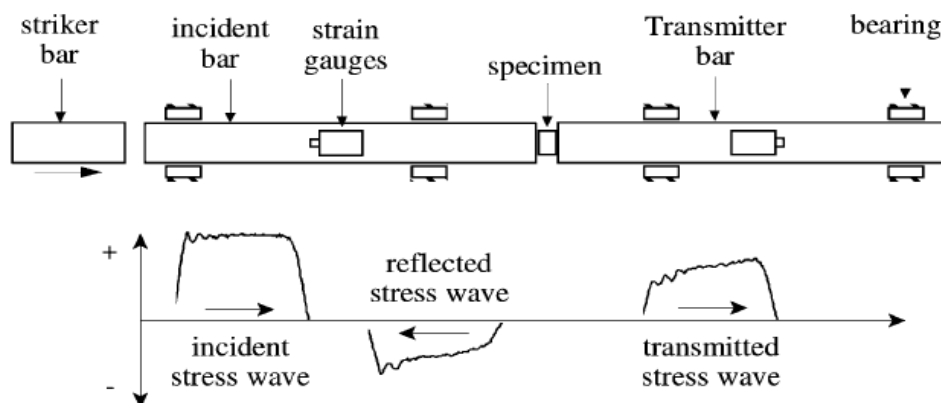
Fig. 9. Schematic drawing of SHPB test equipment, with visualizing of the stress wave during the test, Jaspers [8]

bar". The specimen is placed between the Incident bar and the Transmitter bar. The test specimen is a short cylindrically shaped part.
In the tests a stress wave is caused by a projectile (the Striker bar) impacting at the far end of the incident bar, as shown in Fig. 9. This compressive wave propagates with the speed of sound through the Incident bar only deforming it elastically. Upon reaching the other end of the bar, the incident wave is partly transmitted to the specimen and partly reflected back into the Incident bar as a tensile wave. While propagating in the specimen, the stress wave causes plastic deformation. The remaining stress wave is transmitted into the Transmitter bar and a part is reflected into the specimen.
The stress waves are measured with strain gauges, which are mounted on the two slender bars. As long as the pressure in the Incident bar and the Transmitter bar is the elastic area, stress, strain and strain-rates can be determined based on the strain historic in the slender bars. To get the influence of the temperature, the test is repeated applying heat to the specimens. The tests are repeated at various temperatures.

3.1.1   Argument for using the Johnson-Cook material model

According to the literature survey, the Johnson-Cook material model is the model which has showed the best results in simulating Metal Cutting. Jaspers [8] has achieved good agreement between analyses and tests when using the material model with the material AL 6082-T6, which is used in this work. The Johnson-Cook material model is implemented in LS-DYNA as *0015 "MAT_JOHNSON_COOK".

4   SPH Cutting Model

In this section the model and sensitivity analyses for the model are described. The SPH cutting model is prepared for analysis in the FEM code LS-DYNA. The goal was to obtain a model with a calculation time as short as possible and which is able to predict the force output in agreement with forces measured from experiments, and simultaneously predict a realistic chip formation. The SPH model used was a 3D particle model where the force output was examined in two directions: the cutting force direction and the thrust force direction. The analysis was performed with a constant speed of the tool in the *x* direction, as shown in Fig. 10.

The Tool in the analysis has the same geometry as the tool used in the experiments. A comparison between the numerical analysis and the experiments is described in Section 5.

The following approach based on the literature survey is chosen for the analysis: Several assumptions were made in order to reduce the model size and the computation time, allowing the development of a useful method:

The developed model, a 3D model, is implemented in an orthogonal cutting framework. The model is in modelled in 3D and not 2D to keep the possibility for further expansion of the model to an oblique
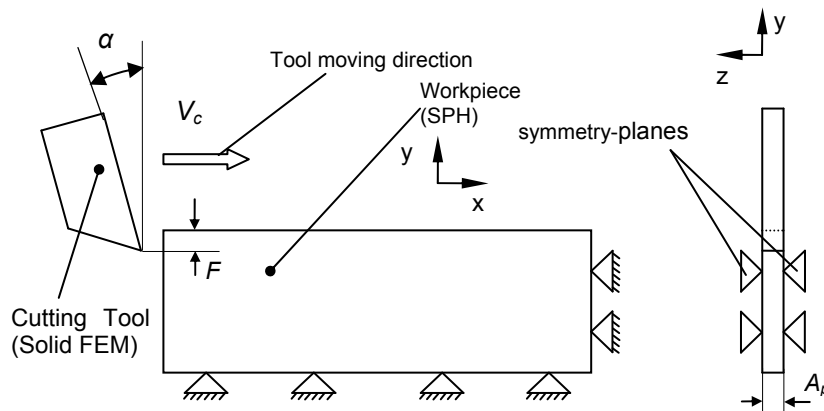
Fig. 10. The SPH model with constraints and nomenclature, V_c: cutting speed, F: cutting depth, A_p: cutting width, α: rake angle

cutting model in future work. In the analyses explicit time integration was used. The computation time was reduced by using process time scaling. The tool velocity used was ten times higher than the real velocity. This technique was used in all simulation in this work, except the sensitivity analysis where the influence of process time scaling was examined and the analysis in section 6.

Consistent units:
In these analyses a consistent set of units were used, namely, cm, g, μs. LS-DYNA requires a consistent set of units to be used. In the first analyses the unit system (mm, tonne, Newton, second) was used but it showed a rounding off error in the analyses. By using (cm, gram, microsecond) instead, the numerical error in each time step was reduced. Changing the unit from second to microsecond, the time step was a larger numerical Figure. and the rounding of error was reduced.
Element formulation:
In these analyses SPH particles were used for the workpiece and Lagrangian 8 nodes constant stress solid elements were used for the tool (*ELEMENT_SOLID: ELFORM 1).
Contact: In these analyses the contact algorithm *CONTACT_AUTOMATIC_NODES_TO_SURFACE was used between the cutting tool and the workpiece. The tool was the master and the workpiece (SPH) was the slave.

Boundary conditions: In these analyses the workpiece was constrained as shown in Fig. 10 applied by *CONSTRAINED_ GLOBAL. The cutting speed was imposed to the cutting tool by *BOUNARY_ PRERIBED_MOTION _RIGID" and *DEFINE CURVE.*

Material formulation:
In these analyses the material model *015 MAT_JOHNSON_COOK was used for the workpiece in LS-DYNA. This material model needs a Equation Of State. *EOS_LINEAR_POLYNOMIAL was used setting C1 to the bulk modulus and all the other C terms to zero. The parameters for material AL 6082-T6 used in these analyses are adapted from Jaspers [8]: A= 428.5 MPa, B=327.7 MPa, n=1.008, C=0.00747, m=1.31. The cutting tool is supposed to be perfectly sharp and rigid (no deformation) and the material model *MAT _020_RIGID" was used

Cutting parameters:
In these analyses the following cutting parameters were used: Cutting depth F = 0.234 mm, Cutting width Ap = 0.20 mm and Cutting speed V_c = 5m/s (when process time scaling is used V_c = 50m/s) and the rake angle of the cutting tool was $α$=0 degrees, see Fig. 10

Computer equipment:
The computer used in these analyses was Sunfire V20Z equipped with 2 pieces AMD Opteron 250 processors (2.4 GHz) and 4GB Memory (RAM).

4.1   Sensitivity Analyses

Series of sensitivity analyses were performed in order to evaluate the SPH model. A comparison of the influence of the force output between two or more analyses in each specific sensitivity analysis was performed. The same tool geometry, chip depth and chip width were used in the models as in the experiments. Sensitivity analyses must be performed on many parameters, thus due to computation time this work is concentrated on the following:
The force output was examined when the following parameters were changed: Particle resolution, influence of mass-scaling, influence of process time scaling and friction between workpiece and tool. In addition, the following parameters were examined related to the force output: The influence of the MEMORY on the *CONTROL_SPH CARD and the influence of the CLSH on the *SECTION_SPH card, the influence of the interval between data is written to the RCFORC-file, the simulation time (cutting length) and the differences between penalty and soft contact was also examined. The analysis showed that these additional parameters have little or no effect on the force output and therefore these analyses are not described further in this paper.

4.1.1   Sensitivity Analysis of the Particle Resolutions Influence on the Force Output

This sensitivity analysis is a convergence analysis of the particle resolution's influence on the force output. In order to examine the influence of the particle resolution on the force output 9 different analyses were performed. All analyses were made under identical conditions, except the particle resolution. Fig. 11 shows the chip formation from an analysis with 125.000 particles per cm^3.
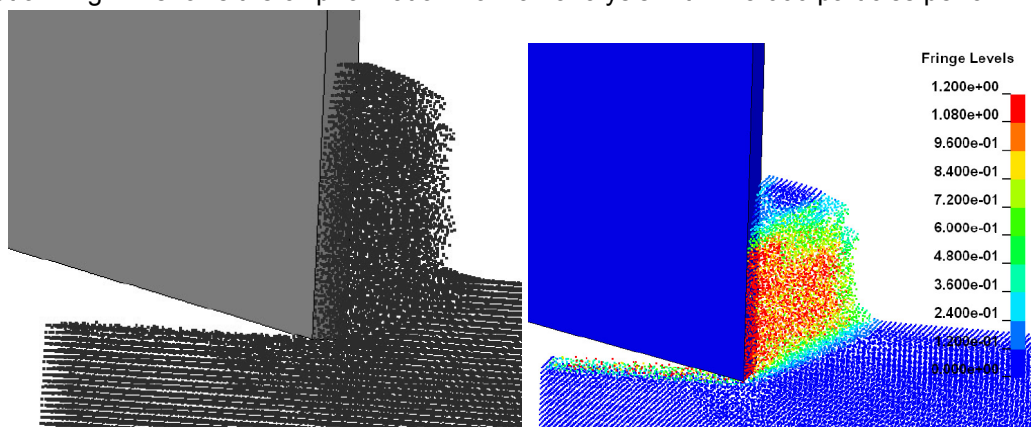
Fig. 11. Chip formation from analysis with 125000 particles per cm^3, calculation time 28 min., 50 sec. Left) 3D view. Right) 3D view: contours of effective plastic strain

The particle resolution of the workpiece was applied by having the same distance between the particles in the chip width, the chip depth and in the moving direction of the tool, see Fig. 10. The static friction coefficient FS and the dynamic coefficient FD were for these analyses both =0.2. The predicted

force output was compared with forces measured in experiments; the experiments are described in section 5.

As shown in Fig. 12 the cutting force converged to a constant level already at a low particle resolution.
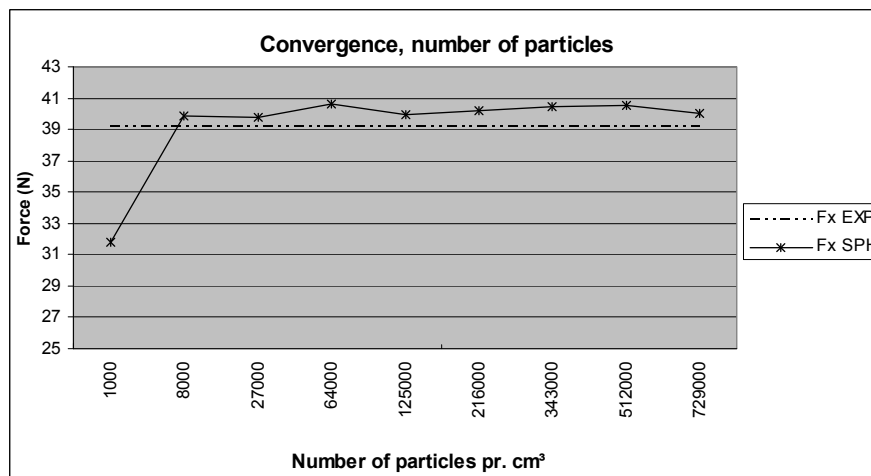
Fig. 12. Convergence for the Cutting force F_x as a function of number of particles per cm^3, compared with measured force from experiments

As shown in Fig. 13 the thrust force converged to a constant level already at a low particle resolution.
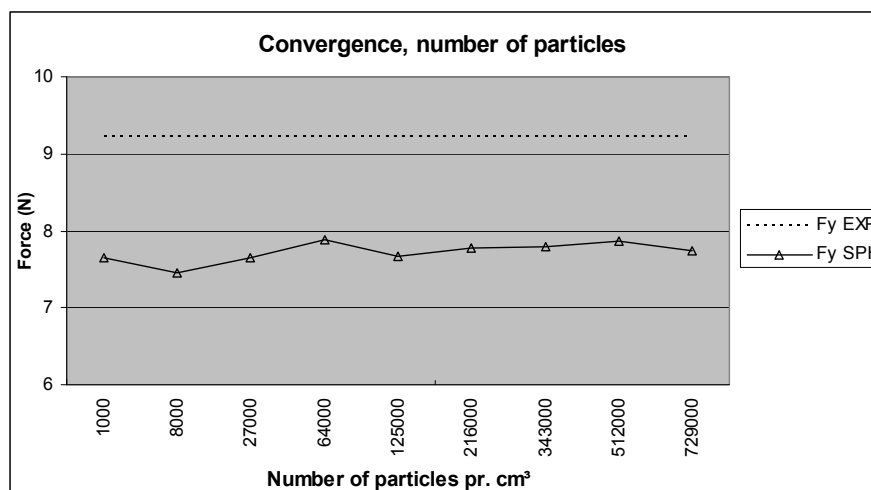
Fig. 13. Convergence for the thrust force F_y, as a function of number of particles per cm^3, compared with measured force from experiments

The conclusion is that the analyses carried out converged to a constant level already at a low particle resolution, and good agreement between predicted force output and forces measured from experiments were achieved.

4.1.2   *Sensitivity Analysis of the Effect of Mass Scaling*

Two analyses were carried out in order to examine the influence of mass scaling on the force output. The two analyses were identical, the only exception was that one was carried out with mass scaling and one was without mass scaling. In the SPH method mass scaling is performed by scaling the mass at each SPH particle, in this case all particles in the workpiece were mass scaled with a ratio = 1.2 The dynamic friction coefficient FD and the static friction coefficient FS, were for these analyses both =0.2.
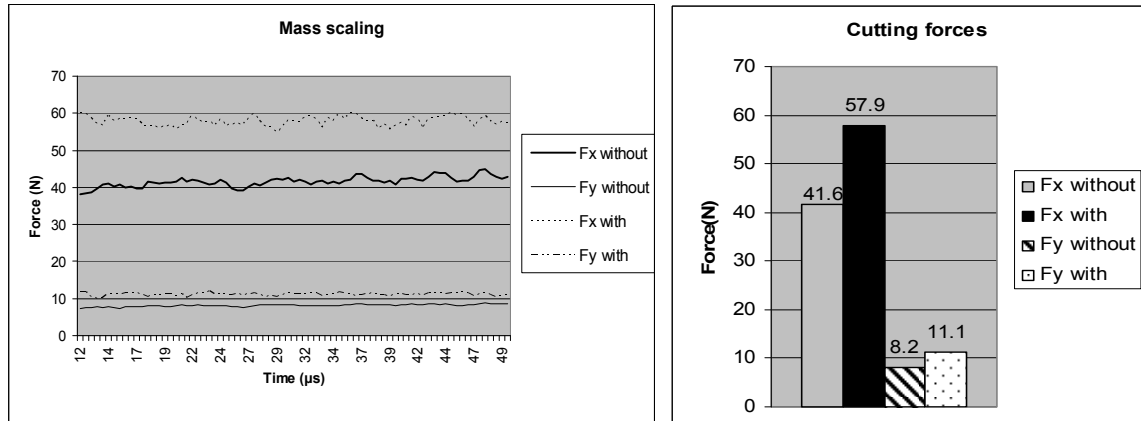
Fig. 14. The simulated forces where the forces have a steady state condition, with and without mass scaling , time interval 12 – 50 µs. left) Force output, right) average values of the forces

The force output from the two analyses is compared in Fig. 14. As shown in Fig. 14 the force output is larger for the cutting force F_x and for the thrust force F_y for the analysis where the mass-scaling technique was used. The calculation time for the analysis was reduced: the computable time was 22 minutes 12 second without mass scaling and 5 minutes and 43 second with mass scaling. As it can be observed from Fig. 14 even a small mass scaling introduces rather large inertia effects, thus mass scaling is not an adequate way of reducing calculation time. Therefore it is not recommended in metal cutting analysis.

4.1.3   Sensitivity analysis of the effect of process time scaling

Five analyses were carried out in order to examine the influence of the effect of process time scaling on the force output. The five analyses were identical except for the variation of the process time. The dynamic friction coefficient FD and the static friction coefficient FS were for these analyses both =0.2. This technique was used in order to reduce the computation time. This technique is usually used in simulation of forming operations. It is valid as long as the accelerated mass is low and the material behaviour is only slightly influenced by the strain rate.

The force output for the five analyses was compared for the cutting forces F_x, see Fig. 15, and the thrust forces F_z, see Fig. 16.
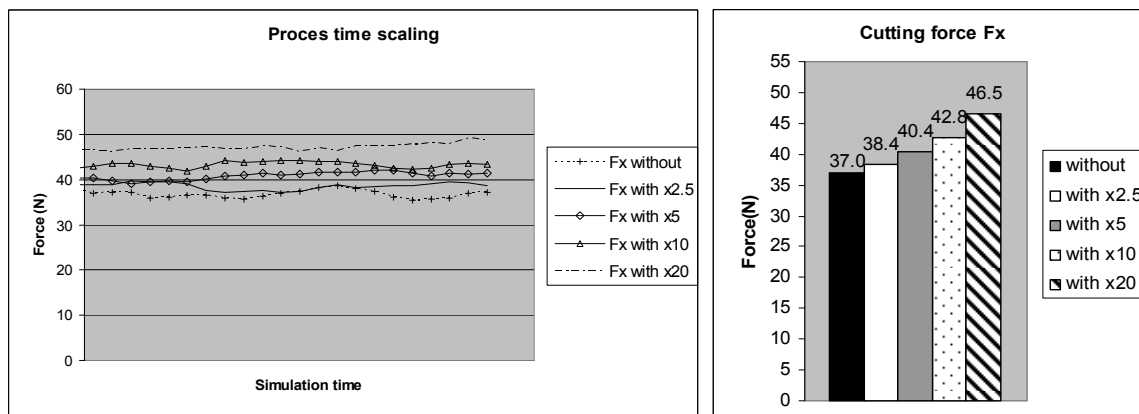
Fig. 15. The predicted cutting forces for different values of the process time scaling. Left) force output. Right) average values of the forces
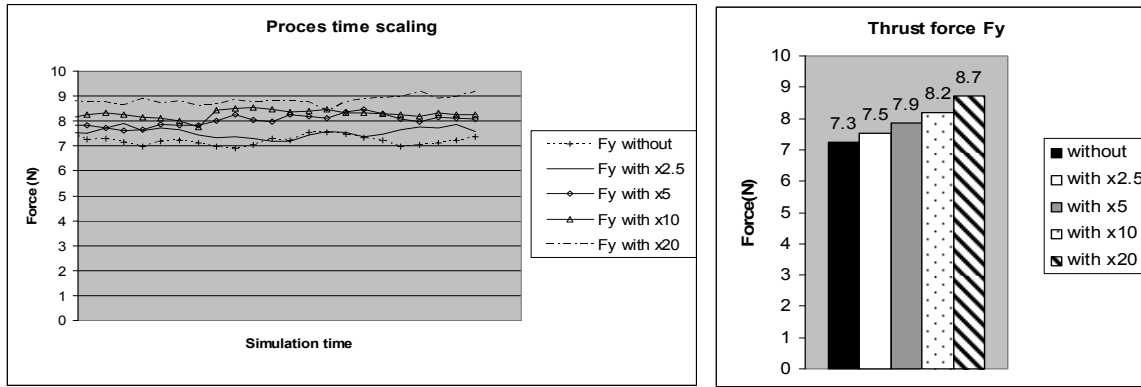
Fig. 16. The predicted thrust forces for different values of the process time scaling. Left) force output. Right) average values of the forces

As shown in Fig. 15 and Fig. 16 the force output for the cutting force F_x and for the thrust force F_z increases approximately proportionally with the process time scaling. This increasing tendency on the force output is related to the addition of the inertia forces. Computation time was reduced from 30 hours and 56 minutes without process time scaling to 1 hour and 51 minutes where the tool velocity is up to 20 times higher than the real velocity.

As shown in Fig. 17 the computation time is reduced significantly when using this technique. The analysis in which a process time scaling factor =2.5 was used, the deviation of the force output compared to the analysis with real velocity were 3.8% for the cutting force and 2.7% for the thrust force. At the same time the computation time was reduced by 51%. The analysis in which a process time scaling factor =5 was used, the deviation of the force output compared to the analysis with real velocity were 9.2% for the cutting force and 8.2% for the thrust force. At the same time the computation time was reduced by 87.7%. The performed sensitivity analyses show that the process time scaling technique can be used as a reasonable assumption for the analysis of the cutting process with a velocity 2.5 to 5 times higher than the real velocity. However, the final calculation should always be carried out without process time scaling.

Proces time	Deviations in force output in %		Computation time
scaling factor	for cutting force	for thrust force	reduced in %
without	0.0	0.0	0.0
x2.5	3.8	2.7	51.0
x5	9.2	8.2	87.7
x10	15.7	12.3	92.6
x20	25.7	19.2	94.0
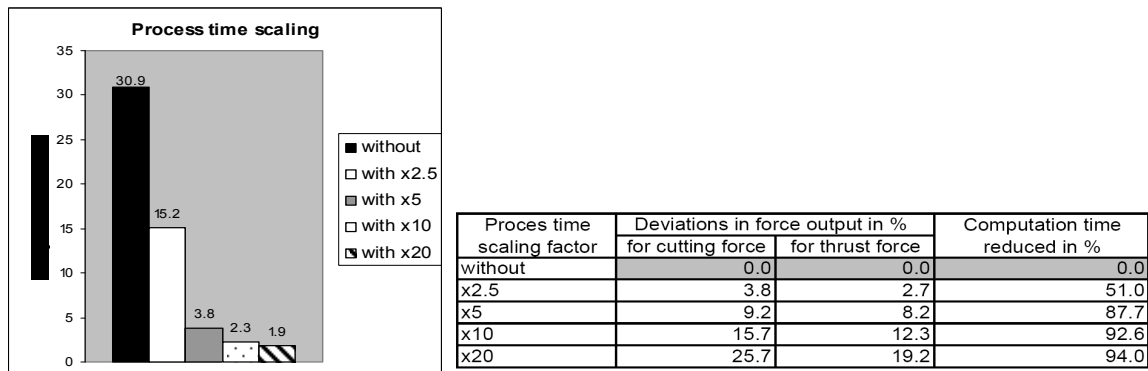
Fig. 17. Left) Computation time, for different values of process time scaling, Right) Table presenting the deviations of the force output and the reduction of computation time compared to the analysis without using the process time scaling technique

4.1.4   *Analysis of Friction between Workpiece and Tool*

In order to examine the influence of friction on the force output, three analyses were carried out. These analyses were identical except for the values of the static friction coefficient *FS* and the dynamic friction coefficient *FD* in LS-DYNA. The friction coefficients *FS* and *FD* are in the following section named *μ* and no distinction will be made between the static and dynamic friction coefficient.

The force output for the three analyses was compared, for the cutting forces F_x in Fig. 18 and the thrust forces F_z in Fig. 19. In order to reduce computation time both analyses were performed by using
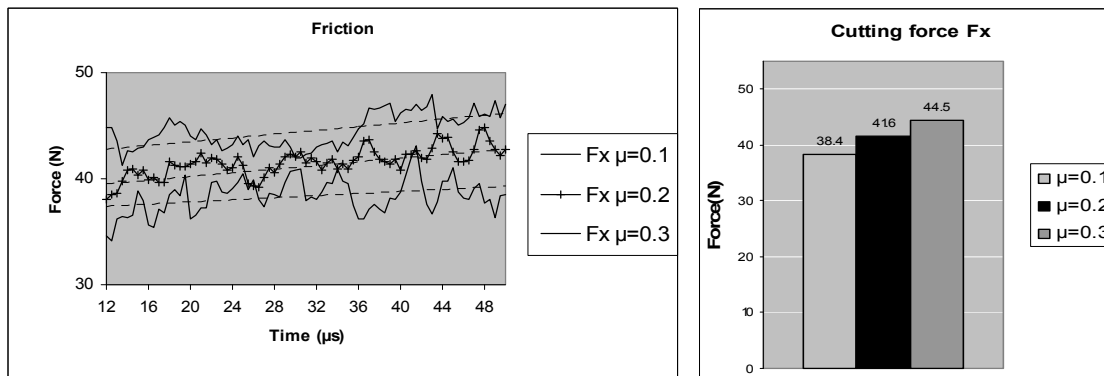
Fig. 18. Predicted cutting force for different values of the friction coefficient μ in the time interval 12- 50 μs. Left) Force output with regression curves, Right) Average values of the forces
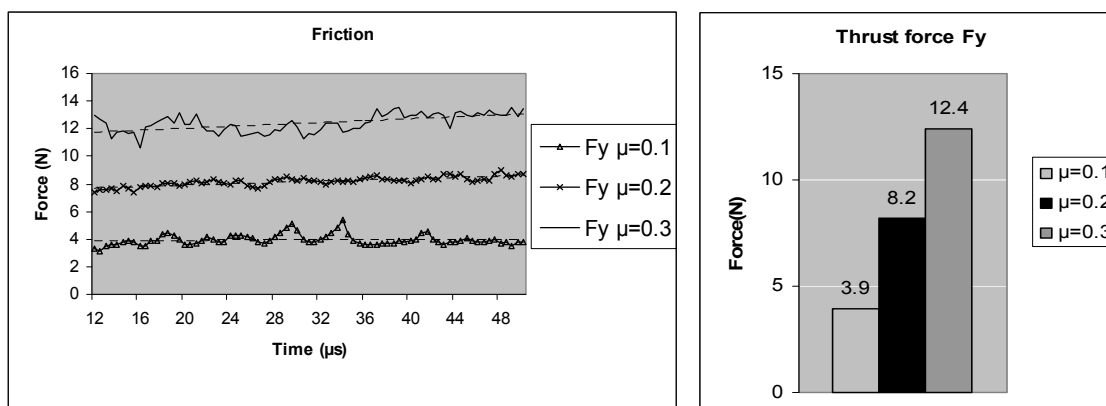
Fig. 19. Predicted thrust force for different values of the friction coefficient μ in the time interval 12- 50 μs. Left) Force output with regression curves, Right) Average values of the forces

the process time scaling technique. The force curves have an increasing tendency due to that the chip is increasing during machining. This is possibly caused by the increasing mass of the chip.
As shown in Fig. 18 and Fig. 19 Frictional behaviour is predicted well. The differences between the force output for the tree analyses are significant. The SPH method predicts the force output proportional to the friction coefficient. Earlier analysis performed by Villumsen and Faurholdt [27] using the Finite Element Method to examine frictional behaviour concludes that the Finite Element Method does not model frictional behaviour well. The conclusion from this analysis is that the SPH method predicts frictional behaviour rather well and considerably better than the Finite Element Method.

5 Experimental Measuring of the Cutting Forces

In order to compare the force output from the numerical analysis and the actual cutting forces, it was necessary to carry out a number of experiments in which the cutting forces were measured. The SPH model was a 3D particle model as earlier described, in which the force output was examined in two directions: the cutting force direction F_x and the thrust force direction F_z. An often applied method to approach the conditions for orthogonal cutting is performed by machining the end of a thin-walled
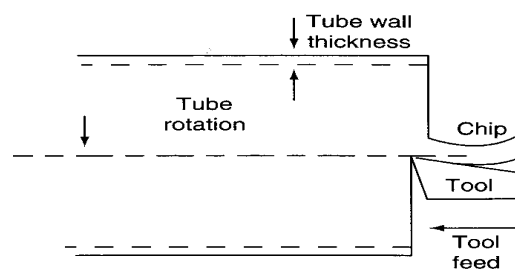
Fig. 20. End turning of a thin-walled tube to approach the conditions for orthogonal cutting, Stephenson and Agapiou [15]

tube. Thus these SPH calculations can be compared with orthogonal cutting with good agreement. This method is used by Merchant [16], Armarego and Brown [10], Oxley [14], Stephenson and Agapiou [15] and Bissacco [13]. An example of this is shown in Fig. 20.

5.1 Test Setup

The test setup in the lathe is shown in Fig. 21. The cutting tool engages with the end of the specimen. Force acquisition was started a few seconds before the beginning of the engagement and was stopped at the end of the test run. The experiments were carried out without cooling and lubrication. Furthermore, the experiments were carried out with the following setup parameters: cutting speed V_c = 300 m/min, feed (chip depth) F= 0.234 mm/rev, chip width (the wall thickness on the tube) A_a= 0.2 mm and average diameter of the tube d_m = 65 mm. The specimen was an extruded aluminium profile, Material EN AW 6082 T6. The extruded specimen is reduced in wall thickness from 5 mm to 0.2 mm applied by turning before carrying out the experiments. The cutting forces were measured with a Kistler dynanometer type 9257BA and data from the measuring was stored in a PC. The Dynamometer was mounted on a console in the machine.

The main spindle gives the movement in the machine x and z directions, as shown in Fig. 21. Please
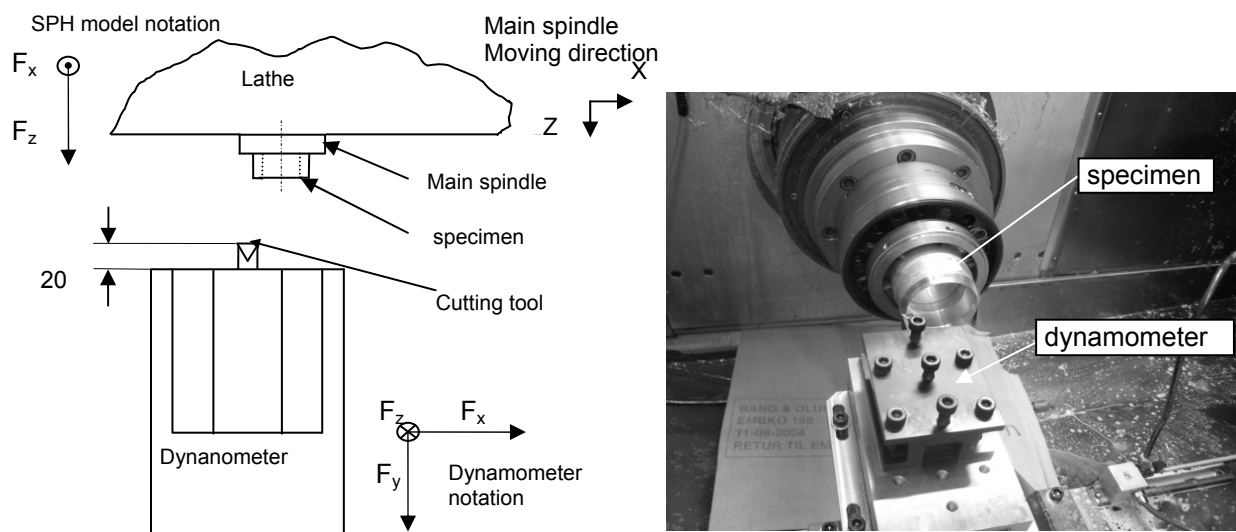
Fig. 21. The test setup, left) schematic drawing of the test setup in the Lathe, right) picture of test setup in the Lathe

note the different coordinate systems for the lathe, the dynanometer and the model.

In order to satisfy statistical demands, the experimental settings were made with five repetitions of each measure-cycle. The measured cutting forces, which were to be compared with the force output from the numerical analysis, were in this case taken when the measured force became a steady state condition, see Fig. 22.

When the measured raw-data was filtered, the average value was calculated for the time region between the two vertically lines, see Fig. 22, where the cutting force was in a steady state condition. Each of these average values represents a measure-value. The five repetitions of the measured
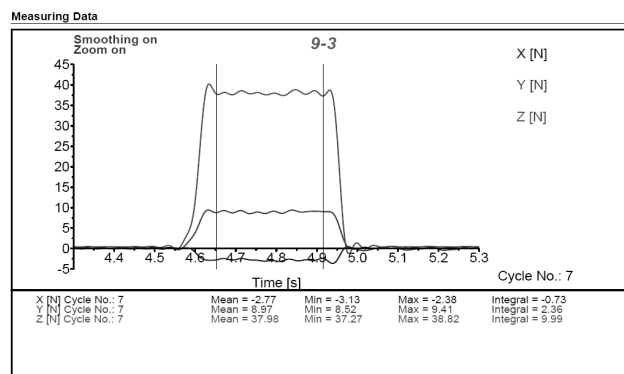
Fig. 22. Typical measure-cycle, steady state condition is between the two vertically lines

forces from the experiment are shown in Table 1 .
The average value of the five measured values was calculated in two directions, the cutting force direction F_x and the thrust force direction F_z. The measured cutting forces were compared with force output from the analysis.

Test no.	Vc (cutting speed)	F(cutting depth)	Aa (chip width)	1 Fz1	1 Fx1	2 Fz2	2 Fx2	3 Fz3	3 Fx3	4 Fz4	4 Fx4	5 Fz5	5 Fx5	average values Fz	average values Fx
	m/min	mm/rev	mm	N	N	N	N	N	N	N	N	N	N	N	N
9 3	300	0.234	0.2	10.29	41.78	9.15	39.34	9.16	38.99	8.76	38.1	8.72	37.79	9.22	39.20

Table 1. The test settings and the measured cutting forces

Measured cutting force F_x = 39.2 N, measured thrust force F_z = 9.2 N

6 Comparison Between Experiments and Analysis

In this section an analysis is presented and the force output from this analysis and force output measured from experiments were compared. At the same time a realistic chip formation could be found. The dynamic friction coefficient FD and the static friction coefficient FS, are for this analysis both =0.23. The particle resolution for this analysis was 512.000 particles per cm^3 and the computation time was 31 hours 43 minutes.
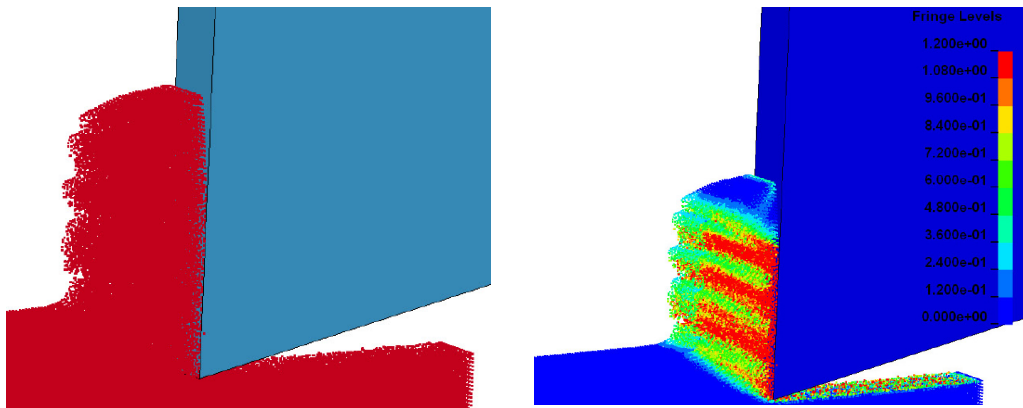
Fig. 23. chip formation from the analysis. Left) 3D view, Right) 3D plot: contours of effective plastic strain

 The aluminium alloy used in this work, AL 6082-T6, is known to produce a continuous chip in the speed and feed range studied in this work. As shown in Fig. 23 the chip formation is realistic in comparison with the chip formation from the experiments. The tool separates the chip from the workpiece in a natural manner and produces a continuous chip.
As shown in Fig. 24 the cutting force F_x and the thrust force F_z lie on an approximate constant level. When the average values from the analysis are compared with the measured forces from the experiments, the following results are achieved. The cutting force F_x is underestimated by 8.4 % and
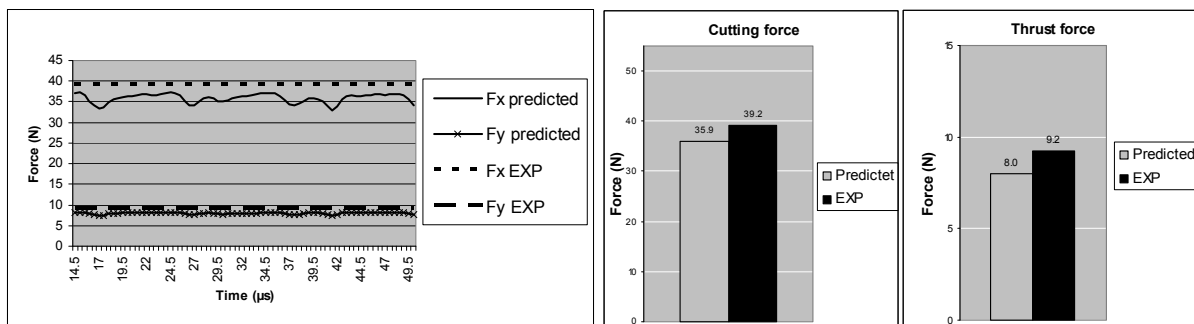
Fig. 24. Cutting forces from the analysis compared to measured cutting forces from experiments. Left) Force output, Right) Average values of the forces

the thrust force F_y is underestimated by 12 %, compared to forces measured from the experiments. In

this work the focus was on the cutting force, because it is this force which typically is the most important regarding fixation in the lathes and the milling machines.

By adapting the friction parameter by a parameter study it is possible to align the differences, at a higher value of the friction coefficient, the cutting force and the thrust force would increase. The cutting force and the thrust force would then be less underestimated.

7 Conclusion

Series of sensitivity analyses were performed and reported in this paper. The force output was examined when the following parameters were changed: Particle resolution, influence of mass-scaling, influence of process time scaling and friction between workpiece and tool.

Particle resolution:
The sensitivity analysis showed that both the cutting force F_x and the thrust force F_y converge to a constant level already at a low particle resolution and good agreement between predicted force output and forces measured from experiments was achieved.

Influence of mass scaling:
When SPH particles are mass scaled the force output is raising when applying mass scaling. The force-output from the two analyses without mass scaling was larger compared to the analysis in which the mass-scaling technique was used. The calculation time for the analysis was reduced but a small mass scaling introduces rather large inertia effects, thus mass scaling is not an adequate way of reducing the calculation time. Therefore, it is not recommended in metal cutting analysis.

Process time scaling:
The cutting force F_x and for the thrust force F_y increase approximately proportionally with a higher process time scaling. This increasing tendency on the force output is related to the addition of the inertia forces. The computation time was reduced from 30 hours and 56 minutes without process time scaling to 1 hour and 51 minutes when the tool velocity was up to 20 times higher than the real velocity. The performed sensitivity analysis showed that the process time scaling technique could be used as a reasonable assumption for analysis of the cutting process with a velocity 2.5 to 5 times higher than the real velocity. However, the final calculation should always be carried out without process time scaling.

Friction between workpiece and tool:
Frictional behaviour was predicted very well, the difference between the force output for the friction coefficient µ=0.1, µ=0.2 and µ=0.3 was significant and the effect of friction was well predicted both for the cutting force and for the thrust force. The SPH method predicts the force output proportional to the friction coefficient. An earlier analysis performed by Villumsen and Faurholdt [27] using the Finite Element Method to examine frictional behaviour, concludes that the Finite Element Method does not model frictional behaviour well. The conclusion from this analysis is that the SPH method predicts frictional behaviour rather well and considerably better than the Finite Element Method.
However, further studies have to be carried out to determine a friction coefficient.

Comparison between experiments and analysis:
In this section an analysis is presented and the force output from this analysis and force output measured from experiments were compared, at the same time a realistic chip formation could be found. The cutting force F_x was underestimated by 8.4 % and the thrust force F_y was underestimated by 12 %, compared to forces measured from the experiments. In this work the focus is on the cutting force, because it is this force which typically is the most important regarding fixation in the lathes and the milling machines. By adapting the friction parameter by a parameter study it is possible to align the differences, at a higher value of the friction coefficient the cutting force and the thrust force will increase. The cutting force and the thrust force will then be less under-estimated.

The overall conclusion is that prediction of cutting forces with the SPH method is realistic and at the same time the chip formation is also predicted realistically.

Future work:
Future work will be concentrated on examination of chip formation and frictional behaviour in metal cutting. Furthermore, the possibilities in simulation of metal cutting using Smooth Particle Hydrodynamics in milling will be explored. A model with a rotating cutting tool must be used in order to

predict cutting forces in the milling process. Experimental measuring of chip geometry and of the cutting forces in the milling process must also be performed in order to get a realistic comparison between analyses and experiments.

8   References

1. Masillamani, D. and Chessa J., Determination of optimal cutting conditions in orthogonal metal cutting using LS-DYNA with design of experiments,2006, 8th International LS-DYNA users conference.
2. Raczy, A. et al., An Eulerian Finite Element Model of the metal cutting process, 2006, 8th International LS-DYNA users conference.
3. Limido, J. et al., SPH method applied to high speed cutting modelling, International Journal of Mechanical Sciences 49, 2007, pp. 898-908.
4. Sartkulvanich, P. et al., Effects of flow stress and friction models in finite element analysis of orthogonal cutting - a sensitivity analysis, Machining Science and technology 9, 2005, pp. 1-26.
5. Fang, N., A new Quantitative sensitivity analysis of the flow stress of 18 engineering materials in machining. Transactions of the ASME Vol. 127, 2005, pp. 192-196.
6. Özel, T. and Karpat, Y., Identification of constitutive material model parameters for high-strain rate cutting conditions using evolutionary computational algorithms, Materials and manufacturing processes 22, 2007, pp. 659-667
7. Sedeh, A. et al., Extension of Oxley's analysis of machining to use different material models, Transactions of ASME Vol. 125, 2003, pp. 656-666.
8. Jaspers, S., Metal cutting mechanics and material behaviour, Ph.D. T¨thesis, Technishe Universitet Eindhoven, 1999, ISBN 90-386-0950-7
9. Johnson, G.R. and Cook, W.H., A constitutive model and data for metals subjected to large strains, high strain rates and high temperatures, Proceedings of the 7th International symposium on ballistics, The Hague, The Nederlands,1983, pp. 541-547.
 10. Armarego, E.J.A. and Brown, R.H., The machining of Metals, Prentice-Hall ENGLEWOODS Cliffs,1969, New Jersey.
11. Strenkowski, J.S. and Carroll, J.T.,   Finite element model of orthogonal metal cutting with application to single point diamond turning, International Journal of Science. Vol. 30, No. 12, 1988, pp. 899-920.
12. Kienzle, O., Die Bestimmung von Kräften und Leistungen an spanenden Werkzeugen und Werkzeugmaschinen, Z-VDI 94,1952, pp. 299-302.
13. Bissacco, G., Surface Generation and Optimization in Micromilling, Ph.D. thesis, Technical University of Denmark, 2004, IPL246.04.
14. Oxley, P.L.B., Mechanics of machining, Ellis Horwood Limited, 1989.
15. Stephenson, D. and Agapiou, S., Metal Cutting Theory and practice, Taylor & Francis, 2006,ISBN 0-8247-5888-9
16. Merchant, M.E., Mechanics of metal cutting process. Journal of Applied Physics, 16.5, 1945, pp. 267-275 and pp. 318-324.
17. Zerilli, F.J. and Armstrong, R.W., Dislocation-mechanics-based constitutive relations for material dynamics calculations, Journal of Applied Physics, Vol. 61, 1987, pp. 1816-1825.
18. Maekawa, et al., Flow Stress of Low Carbon, Steel at High Temperature and Strain Rate Part 2, Flow Stress Under Variable Temperature and Variable Strain Rate, Bull. Jpn. Soc. Precis. Eng., 17, 1983, pp. 167–172.
19. Olovsson, L. et al., An ALE formulation for the solution of two dimensional metal cutting problems, Computer and structures 72, 1999, pp. 497-507.
20. Monaghan, J.J. and Gingold, R.A., Shock Simulation by the Particle Method of SPH, Journal of Computational Physics, 52,1983, pp374-381 and pp. 497-507.
21. Hallquist J., LS-DYNA Theory manual, Livermore software technology corporation, 2006, ISBN 0-977-8540-0-0.
22. Lacome J.L. , Smooth Particle Hydrodynamics Method in LS-DYNA, 3rd LS-DYNA Forum, Bamberg Germany, 2004.
23. Lacome J.L., Smooth Particle Hydrodynamics Method – Part I + II, Livermore software Technology Corporation, 2001.
24. Michel Y. et al., Hypervelocity impacts on thin brittle targets: Experimental data and SPH simulations, International Journal of Impact Engineering 33, 2006, pp. 441-451.
25. Li J. et al., SPH simulation of Hypervelocity Impacts, Journal of Beijing Institute of Technology, Vol.13, No. 3, 2004, pp. 266-269.

26. Chen Y. et al., Experimental Study and Numerical Simulation of Hypervelocity Projectile Impact on double- Wall structure, Journal of Beijing Institute of Technology, Vol.13, No. 3, 2004, pp. 280-284.
27. Villumsen M.F. and Faurholdt T.G., Simulation of Metal Cutting, using the Finite Element Method, a Lagrangian approach, 7th LS-DYNA Forum, Bamberg Germany, 2008,
28. Lucy L.B., A numerical Approach to Testing the Fission Hypothesis, Astronomy Journal, No. 82, 1977, pp. 1013-1024.